JTTEE5 16:580–587
DOI: 10.1007/s11666-007-9050-7
1059-9630/$19.00 © ASM International

Peer Reviewed

Measuring Substrate Temperature Variation During Application of Plasma-Sprayed Zirconia Coatings

H.R. Salimijazi, L. Pershin, T.W. Coyle, J. Mostaghimi, S. Chandra, Y.C. Lau, L. Rosenzweig, and E. Moran

(Submitted February 14, 2007; in revised form April 19, 2007)

Substrate temperature variation was measured during plasma spraying of ZrO_2 7% Y_2O_3 powder using fast-response thermocouples embedded in the stainless steel surface. Coatings were deposited with both stationary and moving torches. The substrate was either kept at room temperature at the start of coating deposition or pre-heated to 270-300 °C. Peak temperature during spraying reached 450 °C for a surface initially at room temperature, and 680 °C for a surface preheated to 300 °C before coating deposition. Preheating the substrate reduced coating porosity by approximately 40%. The porosity at the center of the deposit was significantly lower than that at its periphery since particle temperature and velocity were lower at the edges of the plasma plume than along its axis. When a coating was applied with a moving torch the substrate temperature did not increase above 450 °C, at which temperature heat losses to the ambient equalled the heat supplied by the plasma plume and particles. Coating porosity decreased with distance from the substrate. As sequential layers of coating are applied surface temperature increases and roughness decreases. Both of these factors suppress break-up of particles landing on the substrate and thereby reduce coating porosity.

Keywords porosity of coatings, preheating of substrate, roughness effects, substrate temperature during TS process

1. Introduction

The spread and solidification histories of sprayed particles have a strong effect on the microstructure and physical properties of thermal-sprayed coatings (Ref 1, 2). Experimental studies have shown that in-flight particle characteristics such as temperature and velocity and substrate surface temperature influence the dynamics of particles impact on the substrate in a thermal spray (Ref 3-6). The morphology of molten particles landing and freezing on a flat surface changes from fragmented splats to disk-shape splats with increase of substrate temperature (Ref 5-11). Experiments have shown that when YSZ particles are sprayed on substrates at temperatures above 300 °C, the majority of splats formed are disk-shaped (Ref 7, 9, 11). Figure 1 shows splats of zirconia plasma sprayed on stainless substrates, which were kept at either 300 or 600 °C. At the lower temperature the splats fragmented and are irregular in shape, while at the higher temperature they are mostly disk-shaped.

H.R. Salimijazi, L. Pershin, T.W. Coyle, J. Mostaghimi, and **S. Chandra,** Centre for Advanced Coating Technologies, University of Toronto, Toronto, ON, Canada; **Y.C. Lau, L. Rosenzweig,** and **E. Moran,** GE Global Research, Niskayuna, NY, USA. Contact e-mail: jazi@mie.utoronto.ca.

It has been suggested that the change in splat shape on hot substrates was due to improved contact between the droplet and substrate because condensates and adsorbates on the surface evaporated at elevated temperature, reducing the thermal contact resistance and improving wettability (Ref 3, 7). Splat morphology may also depend on the distribution of particle properties in the thermal spray. Experiments (Ref 11) have shown that as we move from the center to the edge of a plasma plume the average temperature and velocity of the in-flight particles is reduced, and the fraction of splats that splashed and fragmented increased.

Substrate temperature at the point of droplet impact is one of the most important parameters influencing final splat morphology and consequently the properties of the thermal-sprayed coating. Few studies have been done, however, to measure substrate temperature variation during coating deposition, or to correlate it with coating properties. This study was conducted to record the temperature of the substrate/coating interface during plasma spray coating deposition using custom-made, fast-response surface thermocouples. In-flight particle temperatures and velocities were measured in the plasma plume. Deposits were made using a stationary plasma torch so that the effect of particle properties on coating porosity could be correlated.

2. Experimental Procedure

To monitor substrate surface temperature variation, fast-response thermocouples were embedded into the

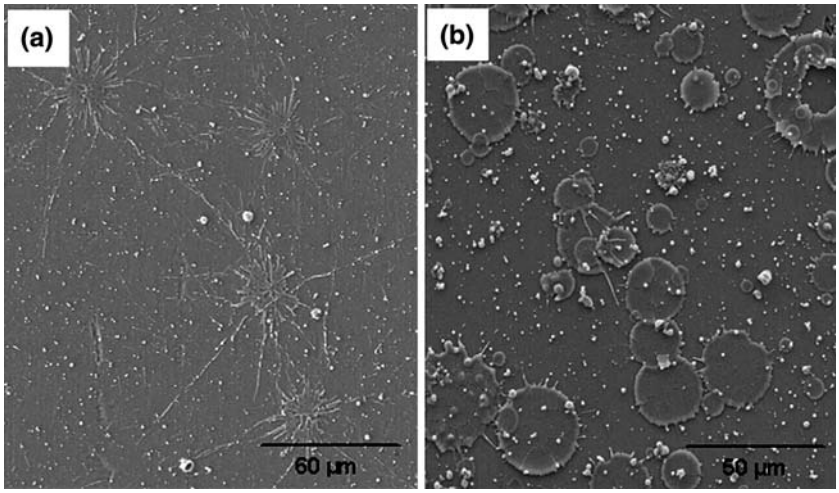

Fig. 1 SEM images of splats deposited on stainless steel substrates initially kept at (a) 300 °C and (b) 600 °C

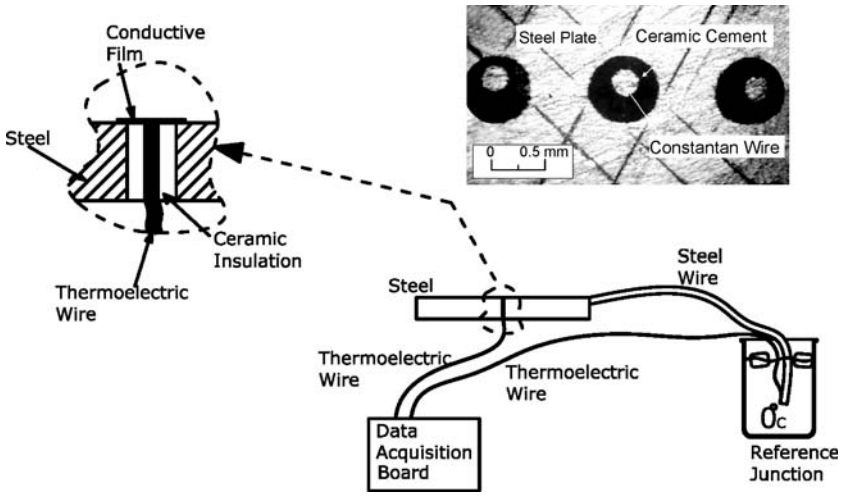

Fig. 2 A schematic diagram of the thin film thermocouple used for temperature evaluation measurement (Ref 8, 9)

substrates made of 304 stainless steel (Fig. 2). The stainless steel substrate acted as one of the thermocouple's electrodes, while the other electrode was a 0.254 mm diameter Constantan wire. The wire was inserted through a 1 mm hole drilled in the substrate and held in place by ceramic cement that also acted as an electrical insulator between the wire and substrate. The inset in Fig. 2 is a top view of three sensors spaced 1.15 mm apart. When a thin metallic bond coat (NiCrAlY) was sprayed on the specimen it formed a junction between the steel and Constantan, creating a thermocouple. The voltage difference between the two junctions, the substrate and wire formed by the bond coat, and another a reference junction kept in an ice bath at 0 °C was recorded as a function of the substrate temperature. The response time of the sensor was confirmed to be less than 40 ns. Detailed descriptions of the thermocouples and calibration procedure have been given elsewhere (Ref 12, 13). A total of seven thin film

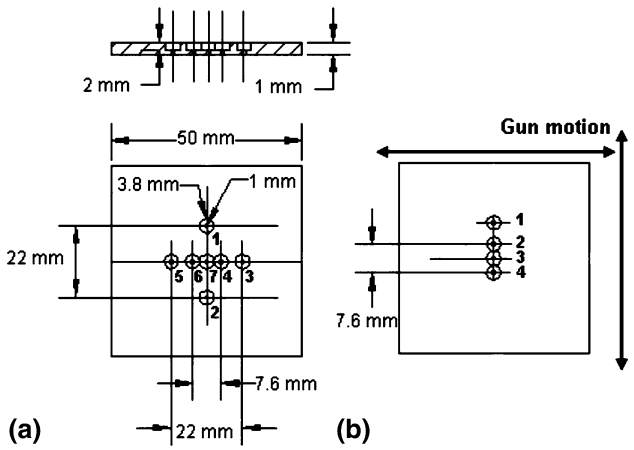

Fig. 3 Footprint substrate dimension and thermocouples locations for (a) stationary footprint and (b) coating deposition

Table 1 Plasma spray parameters

Gun	SG 100
Current, A	630
Voltage, V	41
Total gas flow rate, (Ar/He), slpm	50/20
Feed rate, g/min	8
Spray distance, mm	50

thermocouples were fixed in each specimen (50 mm×50 mm×3 mm) as shown in Fig. 3a. For a second set of tests in which coatings were deposited with a moving plasma torch, four thermocouples were installed (Fig. 3b). All thermocouples were connected to a data acquisition system and 100 samples per minute were recorded during experiments.

In-flight particle conditions were monitored by a DPV-2000 system (Tecnar Ltée, Montréal, QC, Canada). Particle velocity and temperature were measured across a cross section of the plasma plume in a plane 50 mm from the torch exit, at 81 points in a 9×9 grid pattern spaced at 5 mm intervals.

Coatings were made using ZrO_2 7% Y_2O_3 powder (Amperit 825-0, H. C. Starck, Germany) with +5/−25 μm particle size distribution. Experiments were carried out using a SG-100 plasma torch (Praxair, Concord, NH, USA) using the spray process parameters listed in Table 1. For preheating or footprint depositions, the substrate was mounted at a spray distance of 50 mm from the stationary gun. A shielding plate was placed in front of the substrate to protect it from the plasma jet before experiments. After stabilizing the plasma plume, the shielding plate was removed for 2-3 s to allow either particles to land on the substrate, or if no powder was fed into the torch, to preheat the substrate. Some substrates were preheated to 270 °C before footprint deposition. Once the desired amount of material had been deposited, the shielding plate was replaced in front of the substrate and the plasma gun shut down.

To deposit a coating, the gun was kept at 50 mm stand off distance and moved with a speed of approximately 10 cm/s in the horizontal direction with vertical steps of 5 mm between sweeps. Some substrates were preheated before coating. The temperature was raised to approximately 300 °C using four scans of the plasma torch which took a total of 110 s. Then, zirconia powders were injected and a 400-μm thick coating was deposited in 52 layers. In order to study the effect of coating thickness on surface roughness, several coatings were made with thicknesses ranging from 5 to 120 μm. All coatings were made on the grit blasted stainless steel substrates initially kept at room temperature. Surface roughness of coatings was measured by a surfometer (Precision Devices Inc., MI, USA).

Cross sections through the footprints and deposits were polished and examined under a scanning electron microscope (Hitachi-S570) and an optical microscope (Nikon Measurescope). Coating porosity was measured using image analysis software (Optimas6, Media Cybernetics, Silver Spring, MD, USA).

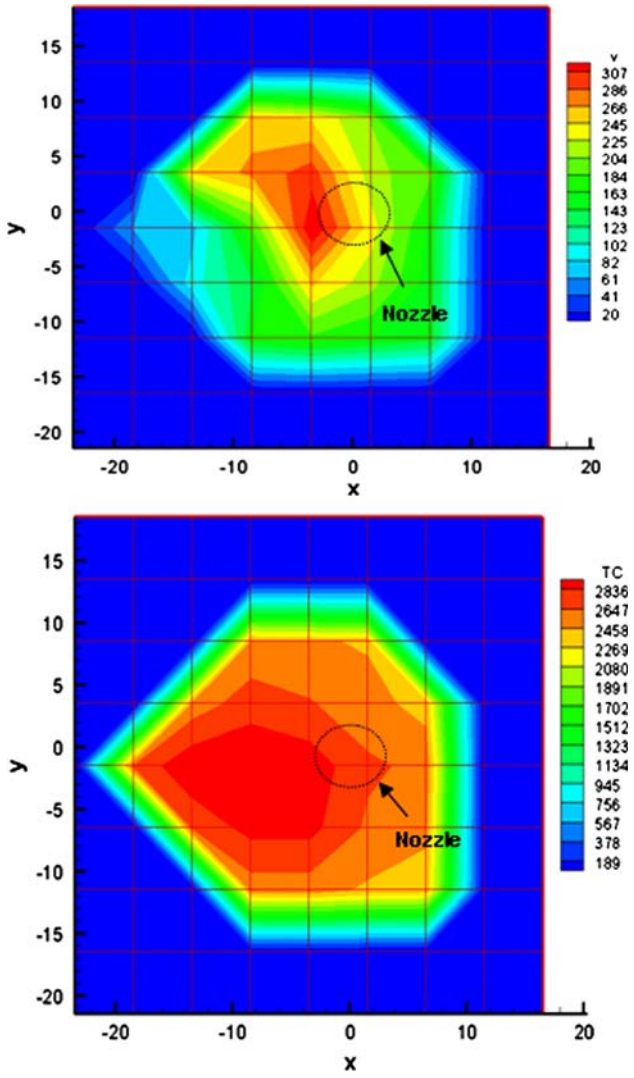

Fig. 4 Particles velocity and temperature within the plasma plume at 50 mm spray distance

3. Results and Discussion

3.1 Temperature Measurements

Figure 4 shows the variation of particle temperature and velocity measured using the DPV-2000 at a distance of 50 mm from the torch nozzle exit. After injecting the powder, the average particle temperature and velocity in the center of the plume were 2752 °C and 237 m/s, respectively. The center of the particulate plume, defined by the points of maximum velocity and temperature, did not coincide exactly with the axis of the nozzle.

Figure 5 shows photographs of the footprints deposited by a stationary plasma torch on substrates that were initially either at room temperature (Fig. 5a) and then exposed to the particle spray for 2.1 s, or first preheated to 270 °C by exposing it to the plasma plume, and then coated for 2.8 s (Fig. 5b). The center of the footprint did not coincide with the gun axis due to interaction of the

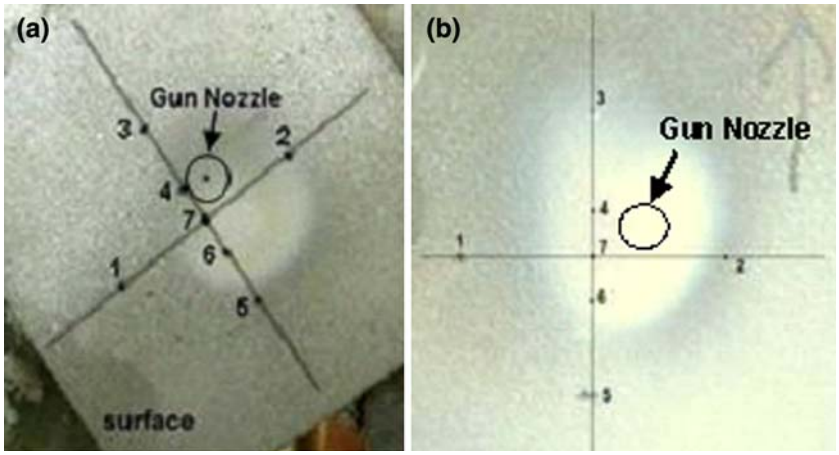

Fig. 5 Deposited footprints and center of the plasma plume with respect to the thermocouples locations. (a) Room temperature substrate and (b) preheated substrate

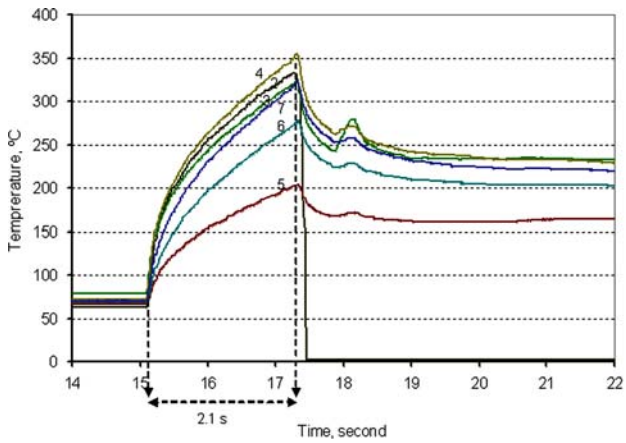

Fig. 6 Temperature evolution during exposure to the plasma plume without powder

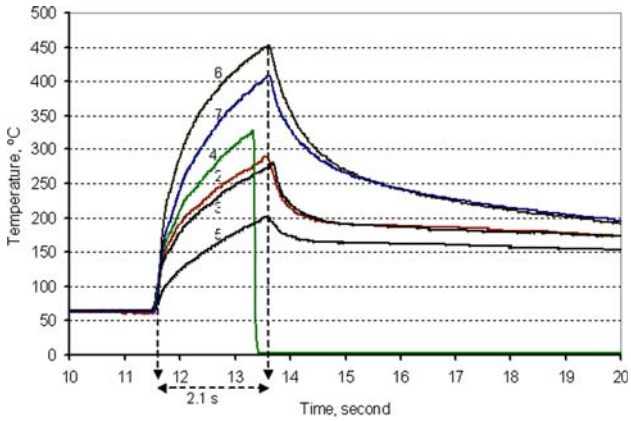

Fig. 7 Temperature evolution during footprint deposition on the substrate at room temperature

injected powders with the tangentional plasma gas flow. The location of the thermocouples embedded in the substrates is shown in both figures.

The temperature of a substrate exposed to a stationary plasma plume for 2.2 s without powder injection is shown in Fig. 6. Thermocouples 4, 2, 3, and 7 were located closest to the center of the plasma plume. The maximum temperature, recorded by thermocouple 4, was as high as 350 °C. There were significant temperature gradients across the surface of substrate. Thermocouple 5, located 11 mm from the center of the substrate recorded a temperature of only 200 °C. After 2.2 s, the shielding plate was placed in front of the substrate and it began to cool. One of the thermocouples (number 2) failed during cooling.

Adding powder to the spray plume greatly increased substrate heating. Figure 7 shows substrate temperature measurements during coating deposition. Except for powder injection, all conditions were the same as those in Fig. 6. The shielding plate was removed for a total of 2.1 s to allow deposition. For 2.1 s, thermocouples 6 and 7 (Fig. 5a) were exposed to maximum heat flow since they were located close to the center of the footprint. One of the thermocouples (number 4) failed during heating and its signal was lost before it reached the peak temperature. These thermocouples recorded peak temperatures of 400-450 °C. Comparison of Figs. 7 with 6 shows that heat from molten particles in the spray increased surface temperature by approximately 100 °C. There were still large temperature gradients across the substrate: maximum temperature varied from 450 to 270 °C. The maximum thickness of the footprint deposited was approximately 300 μm and the average diameter was 15 mm.

To study the effect of preheating the substrate on the substrate/coating interface temperature and on the coating microstructure, the stainless steel substrate was preheated to 270 °C by scanning it with the plasma plume. The torch position was adjusted so that the footprint center was as close as possible to thermocouple 4. The shielding plate was removed for a period of 2.8 s. The footprint deposit and the gun nozzle position are shown in Fig. 5(b). The

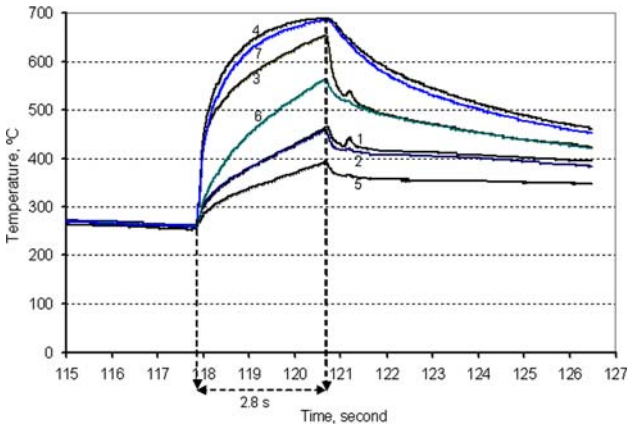

Fig. 8 Temperature evaluation during deposition on the preheated substrate

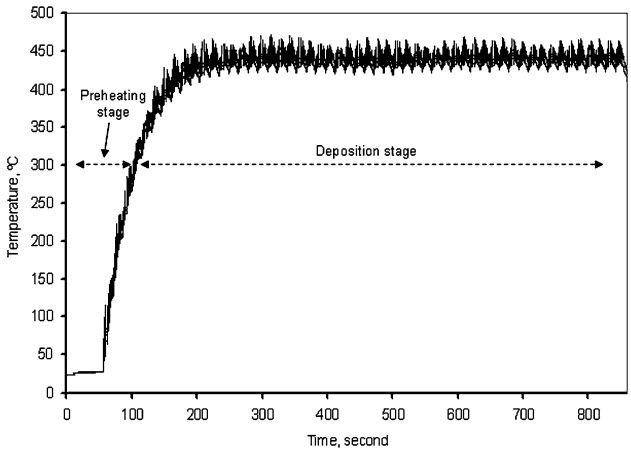

Fig. 9 Temperature evolution during spraying at 50 mm stand off distance

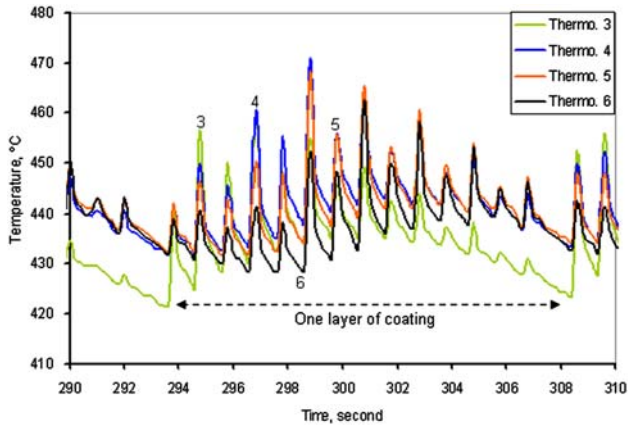

Fig. 10 Expanded area of the stabilized region shown in Fig. 9

temperature variation recorded by the thermocouple array is presented in Fig. 8. Initially, the temperature of the interface increased sharply up to 500 °C. Then, as heat losses from the surface due to convection and conduction to the surroundings increased as the surface got hotter, the temperature approached equilibrium. Build-up of the zirconia coating to its final thickness of about 400 μm also reduced heat conduction into the substrate. The peak temperature reached during coating of the preheated substrate was very high, approaching 700 °C. Once the deposit thickness of about 400 μm was obtained, the interface temperature did not increase further since the substrate was approaching thermal equilibrium, where heat losses to the ambient equaled heat input from the plasma torch.

Temperature measurements during an actual plasma spray coating process with a moving spray torch were also performed in this study. The torch parameters were the same as for the footprint deposits except that the total gas flow rate was increased to 120 slpm. The average temperature and velocity of in-flight particles in the center of the plasma plume were 2600 °C and 460 m/s, respectively. Coatings were deposited on both preheated and non-heated surfaces. In the case on non-heated substrates powder was injected into the plasma plume as soon as it was directed onto the test coupon. Steel substrates were preheated by passing the plasma jet over them before injecting powder. Figure 9 shows the temperature variation during coating application on a preheated surface. No powder was added to the plasma torch during the first four passes until the surface temperature reached approximately 300 °C. Then, zirconia powder was injected while the spray torch scanned back-and-forth across the substrate. The position of the thermocouples on the surface and the direction of gun motion are shown in Fig. 3b.

Starting from the initial temperature of approximately 300 °C, the recorded interface temperature increased rapidly to over 400 °C during the first six layers of coating, reaching a plateau that oscillated between 430 and 460 °C for the remaining 46 passes of the torch (Fig. 9). The peak temperature was significantly lower than that reached with a stationary torch (see Fig. 8), because movement of the torch allowed the substrate to cool. Temperature fluctuations at the interface during deposition of a single layer deposition are shown in Fig. 10, which is an expanded view of a portion of the temperature traces of Fig. 9. The temperature recorded increased rapidly as the torch approached the line of thermocouples (shown in Fig. 3b), reaching up to 470 °C, and then cooled as the plasma plume moved on. As the coating became thicker the amplitude of the temperature oscillations decreased, decreasing from 42 °C at the beginning of the deposition to 22 °C during the last of the 52 layers. The final thickness of the deposited coating was approximately 200 μm.

3.2 Microstructural characterization

Figure 11 shows SEM micrographs of polished cross sections through footprints deposited at room temperature. Images are shown of both the center (Fig. 11a) and a location near the periphery, 7 mm from the center, of the footprint (Fig. 11b). Micrographs illustrate generally good contact between individual particles, with blurred

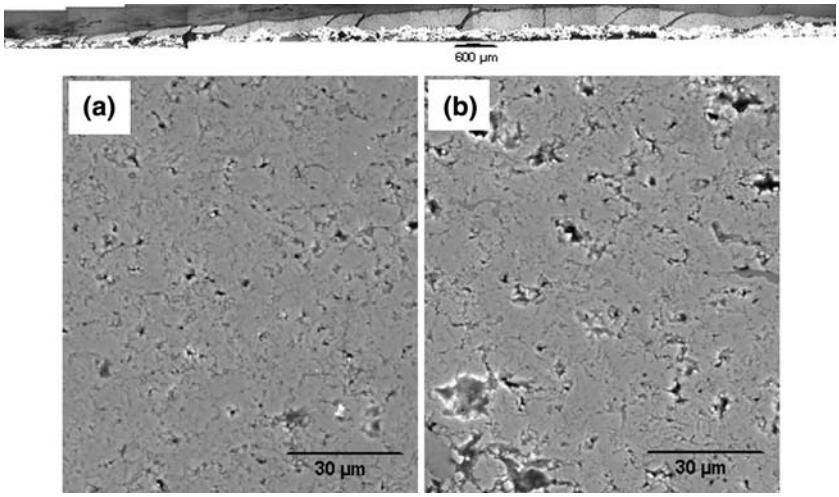

Fig. 11 Micrographs from (a) center and (b) edge of the footprint deposited at room temperature

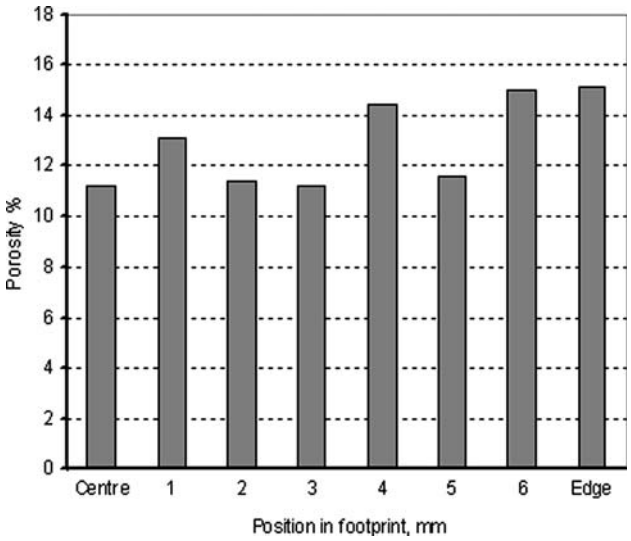

Fig. 12 Porosity distribution of the footprint deposited at room temperature from center to the edge (7 mm from the center) of the footprint

inter-splat boundaries. Pores and microcracks (dark areas) were formed in the microstructure due to gas entrapment and incomplete filling of spaces between splats. Average porosity was measured from such images using image analysis at different locations in the footprint. Figure 12 shows the variation of porosity with location. In general, porosity level at the periphery (7 mm from the center) was higher than at the center of the footprint. The average porosity was 10% in the central region and increased up to 14% at the edges. As shown in Fig. 4, particle velocity and temperature are lower at the periphery of the plasma plume, and fragment upon impact rather than forming disk splats (Ref 11). Particle splashing produces higher porosity since it is difficult to fill in the small spaces at the edges of fragmented splats. A number of vertical cracks through the coating were attributed to high thermal stresses induced by the stationary gun.

Figure 13 shows micrographs through the center (Fig. 13a) and edge (Fig. 13b) of a zirconia coating deposited by a stationary gun on a surface that had been preheated to 270 °C before powder injection into the plasma. Figure 14 shows the distribution of measured porosity as a function of distance from the center of the deposited footprint. The porosity again increased toward the edge of the footprint. However, the level of porosity was much lower than it was on the non-heated substrate, increasing from 4% at the center to 10% at the periphery.

Porosity also varies with depth in a coating. Figure 15a shows SEM micrographs of cross section of YSZ coating made with a moving torch on a stainless steel substrate at room temperature. A horizontal crack can be observed across the coating/substrate interface since no bond coat was used to reduce the thermal expansion coefficients mismatch between the YSZ topcoat and stainless steel substrate. Four different windows, each 40 µm × 40 µm and located at different distances from the coating/substrate interface, were selected for porosity measurement, as marked by rectangles in Fig. 15. Results showed that porosity was approximately 3% close to the interface and reduced gradually to 1% at the top of the coating (Fig. 15a). The procedure repeated for the higher magnification image (Fig. 15b) in three 20 by 20 µm locations and the same trend for the porosity distribution can be seen. It was 3.6% at the interface and reduced to 1.2 and 1.8% as we moved 80 µm toward the upper side of the coating.

Preheating a surface before depositing molten particles on it is known to reduce break-up of splats and coating porosity (Ref 5-11). Heating a surface cleans it of adsorbed contaminants, improving contact between the splat and substrate (Ref 7). The impacting droplet therefore cools rapidly and solidifies before it has time to fragment. This is valid, however, only for the first layer of splats landing on the bare substrate. Subsequent particles land

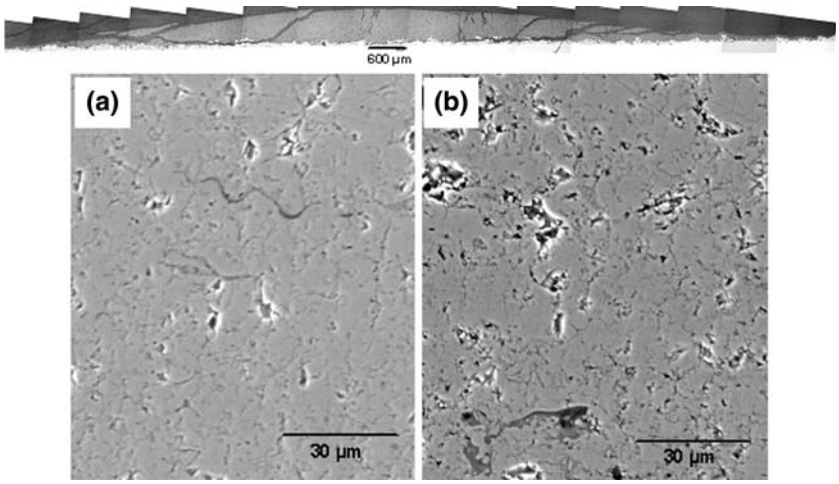

Fig. 13 Micrographs from (a) center and (b) edge of the footprint deposited at 270 °C substrate temperature

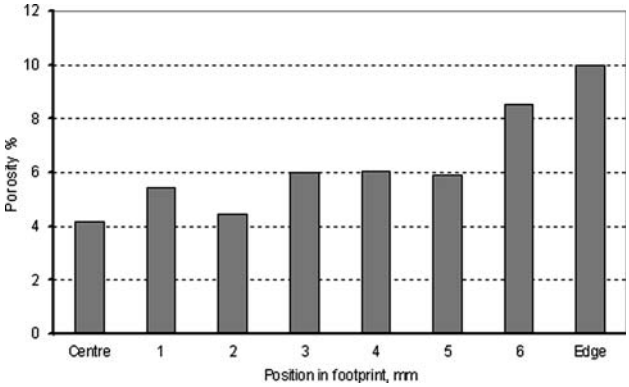

Fig. 14 Porosity distribution in the footprint deposited on the preheated substrate

on an already solidified layer of the coating. It seems plausible, though, that contact between the hot coating and impacting particles is also good, minimizing splashing. The temperature of the coating is approximately 400-450 °C (see Fig. 9), much higher than the transition temperature above which splat fragmentation is no longer observed (Ref 8). Therefore, the porosity would be expected to be lower on the upper layers of the coating than at the substrate-coating interface. Attempts to observe the shape of single splats that had landed on a layer of zirconia were unsuccessful, since it was impossible to identify the boundaries of an individual splat.

Substrate roughness may also be important in promoting porosity: a rough surface increases splat break-up and consequently increases porosity. Tests were done to measure the changes in roughness of the upper coating

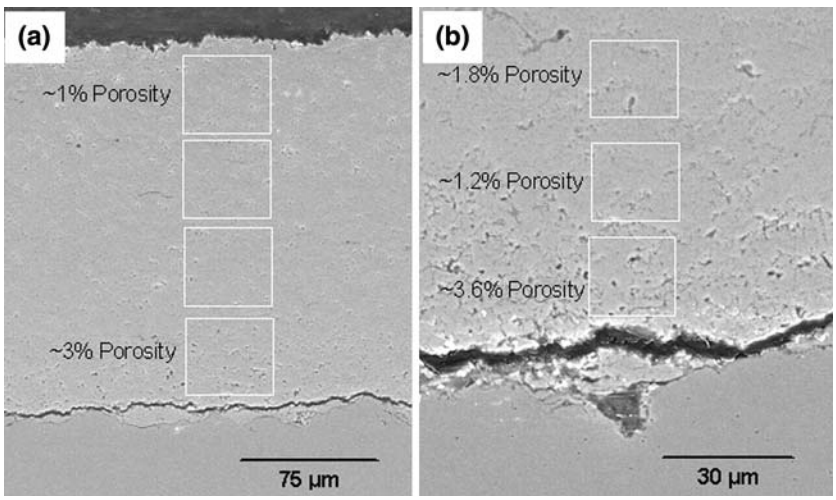

Fig. 15 SEM micrographs of YSZ coating deposited on a stainless steel substrate at room temperature

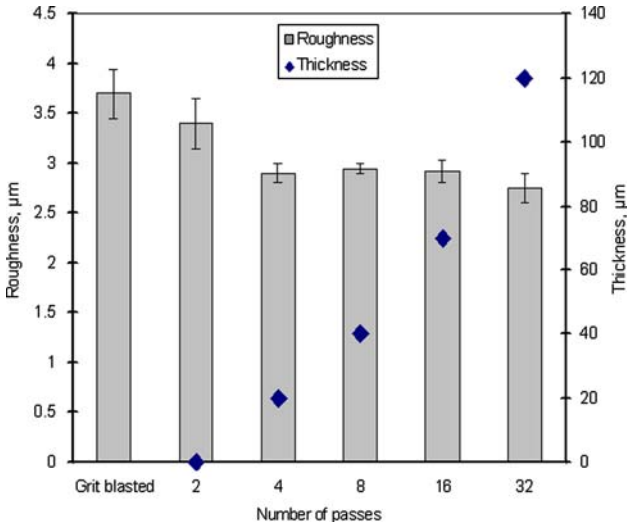

Fig. 16 Surface roughness of YSZ coatings versus deposition thickness

surface as sequential coating layers were applied. A series of coatings were prepared, using 2, 4, 6, 8, 16, and 32 passes of the plasma torch, respectively. Figure 16 shows the surface roughness and thickness of each of the coatings. The initial surface roughness of the grit blasted surface was 3.7 µm and the roughness of the coating decreased as the coating thickness increased. After four passes of the spray torch, which produced a coating approximately 20 µm thick, the value of average surface roughness reached a plateau (2.9 µm) and did not change subsequently. Thus, the coating roughness was less than that of the initial bare surface, and this may have contributed to reducing splat splashing and therefore coating porosity (Ref 14).

4. Conclusions

Surface temperature evolution was measured during deposition of plasma spray coatings using both stationary and moving torches. The substrate was either kept at room temperature at the start of coating deposition, or preheated to 270-300 °C. Peak temperature reached 450 °C for a surface initially at room temperature, and 680 °C for a surface preheated to 300 °C before coating deposition. Preheating the substrate reduced coating porosity by approximately 40%. The porosity at the center of the deposit was significantly lower than that at its periphery since particle temperature and velocity were lower at the edges of the plasma plume than along its axis. When a coating was applied with a moving torch the substrate temperature did not increase above 450 °C, at which temperature heat losses to the ambient equalled the heat supplied by the plasma plume and particles. Coating porosity decreased with distance from the substrate. As sequential layers of coating are applied surface temperature increases and roughness decreases. Both of these factors suppress break-up of particles landing on the substrate and thereby reduce coating porosity.

References

1. M. Fukumoto, H. Nagai, and T. Yasui, Influence of Surface Character Change of Substrate due to Heating on Flattening Behavior of Thermal Sprayed Particle, *International Thermal Spray conference and Exposition*, B.R. Marple and C. Moreau, Eds., ASM International, Seattle, WA, USA, 2006
2. H.R. Salimijazi, T.W. Coyle, J. Mostaghimi, and L. Leblanc, Microstructure of Vacuum Plasma-Sprayed Boron Carbide, *J. Therm. Spray. Tech.*, 2005, **14**(3), p 362-368
3. A. McDonald, M. M. Lamontagne, S. Chandra, and C. Moreau, Photographing Impact of Plasma-Sprayed Particles on Metal Substrates, *International Thermal Spray conference and Exposition*, B.R. Marple and C. Moreau, Eds., ASM International, Seattle, WA, USA, 2006
4. M. Pasandideh-Frad, V. Pershin, S. Chandra, and J. Mostaghimi, Splat Shape in a Thermal Spray Coating Process: Simulation and Experiments, *J. Therm. Spray. Tech.*, 2002, **11**(2), p 206-217
5. M. Fukumoto, E. Nishioka, and T. Matsubara, Flattening and Solidification Behavior of a Metal Droplet on a Flat Substrate Surface Held at Various Temperatures, *Surf. Coat. Tech.*, 1999, **120-121**, p 131-137
6. A. Mcdonald, M. Lamontagne, C. Moreau, and S. Chandra, Visulalization of impact of plasma-sprayed molybdenum particles on hot and cold glass subsytrates, *International Thermal Spray Conference: Plasma Spraying*, E. Lugscheider, Ed., May 2-4, 2005, Basel, Switzerland, ASM International, p 1192-1197
7. X. Jiang, Y. Wan, H. Herman, and S. Sampath, Role of Condensates and Adsorbates on Substrate Surface on Fragmentation of Impinging Molten Droplets During Thermal Spray, *Thin Solid Film*, 2001, **385**, p 132-141
8. J. Cedelle, M. Vardelle, and P. Fauchais, Influence of Stainless Steel Substrate Preheating on Surface Topography and on Millimeter- and Micrometer-Sized Splat Formation, *Surface Coat. Technol.*, 2006, **201**, p 1373-1382
9. S. Sampath, X.Y. Jiang, J. Matejicek, A.C. Leger, and A. Vardelle, Substrate Temperature Effects on Splat Formation, Microstructure Development and Properties of Plasma Sprayed Coatings. Part I: Case Study for Partially Stabilized Zirconia, *Mater Sci Technol.*, 1999, **A272**, p 181-188
10. T. Chraska and A.H. King, Effect of Different Substrate Conditions Upon Interface with Plasma Sprayed—A TEM Study, *Surface Coat. Technol.*, 2000, **157**, p 138-246
11. H.R. Salimijazi, L. Pershin, T.W. Coyle, J. Mostaghimi, S. Chandra, C.Y. Lau, L. Rosenzweig, and E. Moran, Effect of Droplet Characteristics and Substrate Surface Topography on the Final Morphology of Plasma Sprayed Zirconia Single splats, *J. Ther. Spray Tech.*, **16**(2), 2007
12. Y. Heichal and S. Chandra, Predicting Thermal Contact Resistance Between Molten Metal Droplets and Solid Surface, *J. Heat Transfer*, 2005, **127**, p 1269-1270
13. Y. Heichal, S. Chandra, and E. Bordatchev, A Fast-Response Thin Film Thermocouple to Measure Rapid Surface Temperature, *Exp. Thermal Fluid Sci.*, 2005, **30**, p 153-159
14. V. Pershin, M. Lufitha, S. Chandra, and J. Mostaghimi, Effect of the Substrate Temperature on Adhesion Strength of Plasma-Sprayed Nickel Coatings, *J. Ther. Spray Tech.*, 2003, **12**(3), p 370-376